STRUCTURAL, ELECTRICAL AND MAGNETIC PROPERTIES OF THE ($Ce_XFe_{0.05}Mg_{0.95-X}O$) NANO COMPOUND SYNTHESIZED VIA SOL-GEL/AUTO COMBUSTION TECHNIQUE

Tagreed M. Al- Saadi* , Ziad T. Khodair , Ahmed H. Abed****
*Baghdad University / *College of Education* for Pure Sciences - *Ibn Al-Haitham* / Physics Dep. Iraq
** University of Diyala, College of Science, Physics Dep. Iraq
tagreedmm2000@gmail.com

ABSTRACT: *In this work (Ce_x $Fe_{0.05}Mg_{0.95-x}O$) nanoparticles (where x= 0, 0.025, 0.05, 0.075 and 0.10) were prepared by using sol-gel /auto combustion technique. The XRD results showed that all samples are polycrystalline in nature with cubic structure and lattice constant (a) decrease with increasing of Ce content in the samples. The crystallite size found an average size of (14.26 – 25.21 nm) was estimated by using Debye-Scherrer equation. The results of (SEM) showed that the morphology look like irregular aggregated of particles.The analysis of (EDX) confirmed the presence of Mg, Ce, Fe and O ions in the prepared samples. The results revealed that the dielectric loss factor and dielectric constant increase with increasing the content of Ce ion , but the conductivity is inverse that behavior also the results showed that the initial magnetic permeability and relative loss factor were affected by changing the content of Ce ion.*

Keyword: Nano Compound, XRD,SEM, Dielectric Properties, Initial Permeability

1. INTRODUCTION

MgO is Multi-use metal oxides has several applications in many fields such as toxic waste remediation [1], catalysis , antimicrobial materials [2], electrochemical biosensor and refractories [3]. The characteristics of Magnesium oxide depend on the preparation method. There are different methods to prepare magnesium oxide nanoparticles; such as combustion, chemical vapour deposition, sol-gel, precipitation, and many other methods [4,5].

Doped mineral oxide nanoparticles are salutary in a wide diversity of applications such as photodetectors, dilute magnetic semiconductors, optoelectronics [6]. The insulator oxides, Oxide-based semiconductors with dilute magnetic properties and which can show a ferromagnetic with Curie temperature up room temperature.These insulator oxides and Oxide-based dilute magnetic semiconductors display room temperature- ferromagnetic with just a little percent of a relocating- mineral doping such as Co, Ni, Fe, Mn, V, or Cr when grown in powder form, induces an important modification in its electric and magnetic properties, etc. Several models of room temperature- ferromagnetic have been a proposition for these insulators and semiconductors, consists of a new exchanged mechanism including donor electrons in an impurity, [7,8]

The aim of this research is studying the effect of Ce ion on some of the Properties of the ($Ce_xFe_{0.05}Mg_{0.95-x}O$) Nanoparticles synthesized by Sol-Gel Auto Combustion Method.

2. EXPERIMENTAL METHOD

The nanoparticles Ce_x $Fe_{0.05}$ $Mg_{0.95-x}$ O were prepared in a sol-gel method and included several stages, as shown in figure (1) :

The analytical grade of nitrates; $Mg(NO_3)_2 .6H_2O$, $Fe(NO_3)_3. 9(H_2O)$, $Ce(NO_3)_3. 6H_2O$ as a precursor and strict acid $C_6H_8O_7 .H_2O$ was utilized as a fuel. A certain quantity of strict acid and nitrates was dissolved into distilled water to obtain an aqueous solution. The ratio was used of citric acid: nitrates (0.5:1) molar. The number of pH of the solution was adjusted to be 7 using ($NH_4(OH)$).

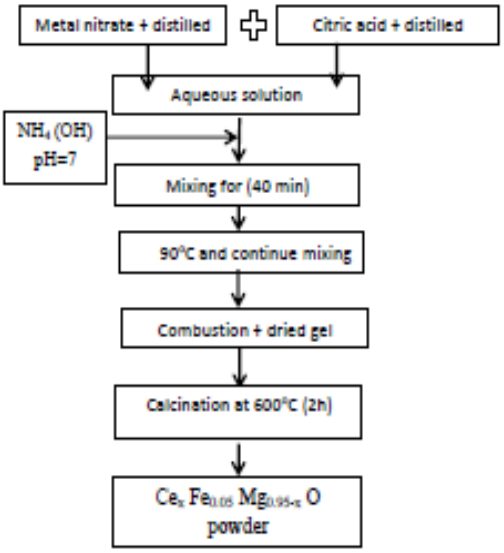

Figure 1: Flow Chart of Preparation

After that, the mixed solution was heated at 90°C with constant stirring. Then, the solution turned from transparent to viscous yellow gel. After that, this gel became dried, then subjected to ignition, followed by combustion, that transformed the dried gel into loose powder within few seconds. The precursor was calcined at a temperature of 600 °C for (2 h) in the air to getting after process be a brown colour. The samples named as P=pure (MgO) , F= ($Fe_{0.05}Mg_{0.95}O$) and D_1, D_2, D_3, D_4= (Ce_x $Fe_{0.05}Mg_{0.95-x}O$) for (x= 0.0, 0.025, 0.05 , 0.075 and 0.1) respectively .

3. RESULTS AND DISCUSSION

1.3. Powder X-ray diffraction Analysis

All the diffraction peaks patterns for all samples are shown in Figure 2 , they indexed according to (JCPDS 45-0946), so that referred to (fcc) structure[9]. These XRD peaks are assigned to (111), (200), (220), (311) and (222) crystal planes and the other peaks referred to the presence of iron and cerium. From Figure 2 can observe the intensity of all the XRD peaks decreases with the addition of Fe and Ce-content and this effect is more clear from the plot of the sample in which Ce-content is x = 0.1.

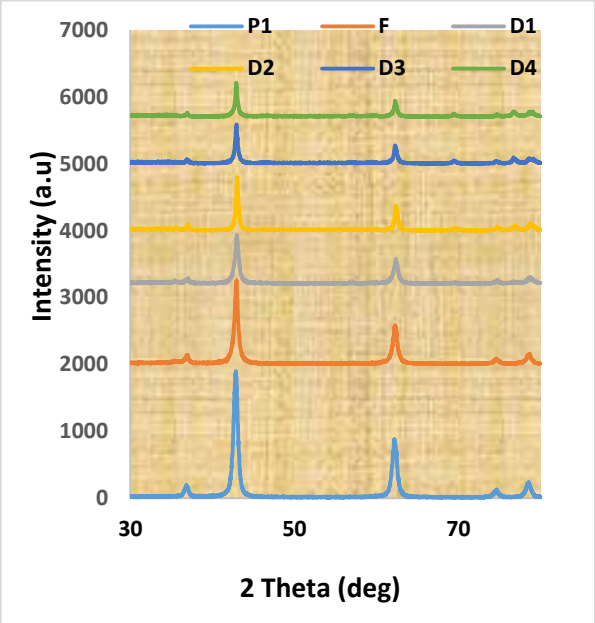

Figure 2: X-ray diffraction pattern of prepared samples

The average crystallite size (D_{av}) of the nanoparticles was calculated using Debye - Scherrer equation.[10]

$D_{av} = K\lambda / \beta \cos\theta$

Where, β: FWHM (full width at half maximum), θ: Bragg's angle , λ: is wavelength and K: is a constant that same to (0.89-0.94) . The calculated (D) , (a) and ($\rho_{x\text{-}ray}$) were given in the table (1) , from this table can observe that when the content of (Ce^{+4}) increased, the XRD lines shifted towards smallest (2θ) angles showing higher values of lattice constant. The shifting of diffraction lines may be attributed due to the difference in size between the (Ce^{+4}) ions (r = 1.01 Å) and (Mg^{+2}) ions (r = 0.86 Å). On the other hand the values of ($\rho_{x\text{-}ray}$) had same behavior of (a) because the density is depend on the value of lattice constant and the molecular weight of the compound [11], But for the sample F the result is opposite because the radius of ion (Fe^{+2}) (r = 0.75 Å) is smaller than the radius of ion (Ce^{+4}).

Table (1) : Variation of Grain size , lattice constant and $\rho_{x\text{-}ray}$ with the Ce concentration.

sample	D(nm)	a(Å)	$\rho_{x\text{-}ray}$ (g/cm^3)	Bulk (ρ) (g/cm^3)	Porosity %
P	13.55	4.2036	3.58	2.77	25.24
F	14.42	4.1999	3.67	2.78	25.27
D1	15.36	4.2055	3.81	2.81	26.32
D2	25.21	4.2077	4.05	3.03	34.98
D3	21.59	4.2080	4.31	2.78	29.15
D4	24.3	4.2185	4.35	2.80	31.46

2.3. SEM and EDX analysis

The microstructure and morphological studies were carried out using a scanning electron microscope (SEM). The images of P, F, D_1 samples are shown in Figures (3a) respectively. From this figures can show irregular aggregated particles, that may be due to the high surface energy possessed by small particles or because of difficulties connected with getting higher magnification [12,13]. The EDX spectra in Figures 3(b) acquired for same samples indicated to the presence of Mg has seen at (1.25 KeV), O at (0.525 KeV), Ce at (0.884KeV) and iron at (0.705 KeV).

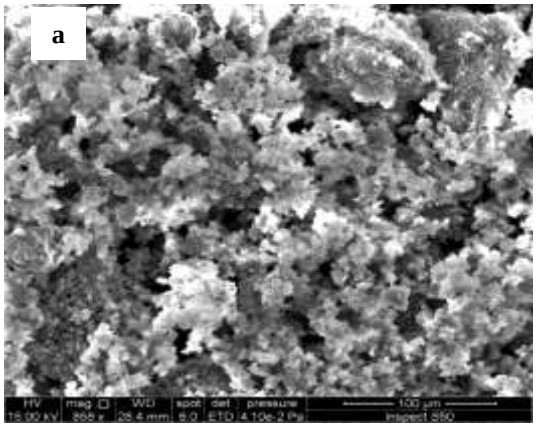

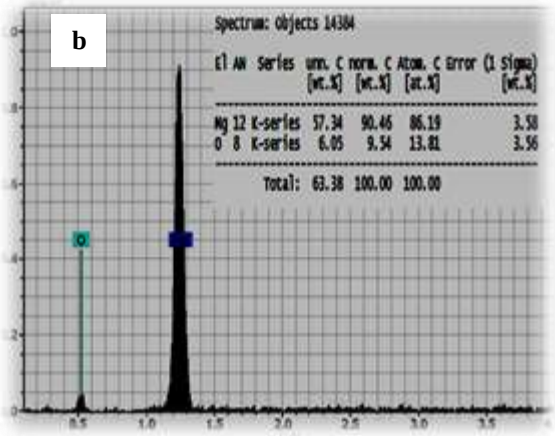

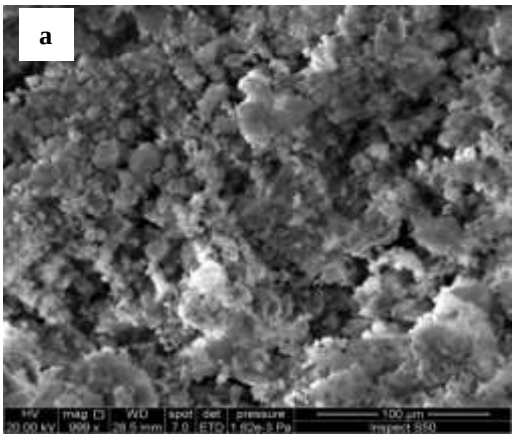

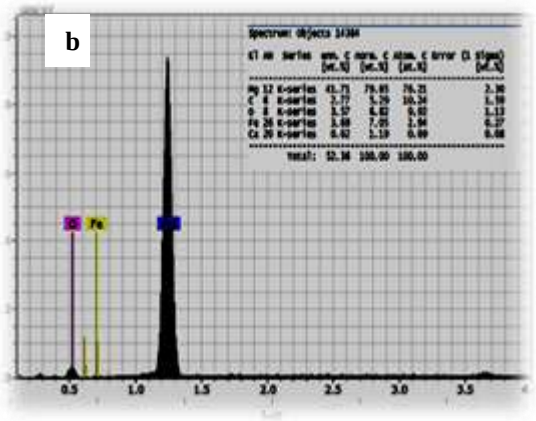

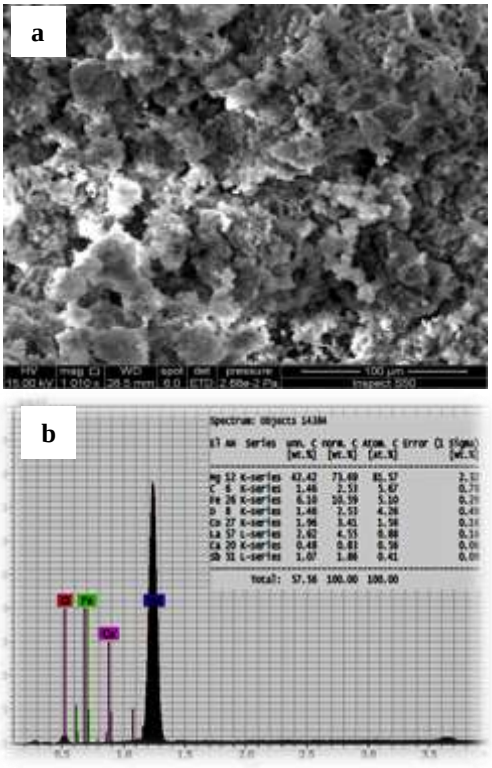

Figure (3): (a)The SEM (b)The (EDX) of the samples P , F and D_1.

3.3.. Dielectric Properties

There are three parameters that affected to choose the materials for suitable devices applications, they are; dielectric constant, dielectric Loss and capacitance. The dielectric constant is given by formula:[14]

$$\varepsilon' = C\,d/\varepsilon_o A$$

Where: (d) the thickness of the dielectric sample, (C) the capacitance, (A) the area of the dielectric material and (ε_o) the permittivity of free space. The variation of dielectric constant (ε_r) with applied frequency for the various compositions of the samples has taken at room temperature and the results are shown in figure 4. This may be attributed to the charge lattice defects (the space charge polarization). The bigger values of dielectric constant at few frequencies may be due to the lowest electrostatic binding strength which arises near from the grain boundary surface [15] .

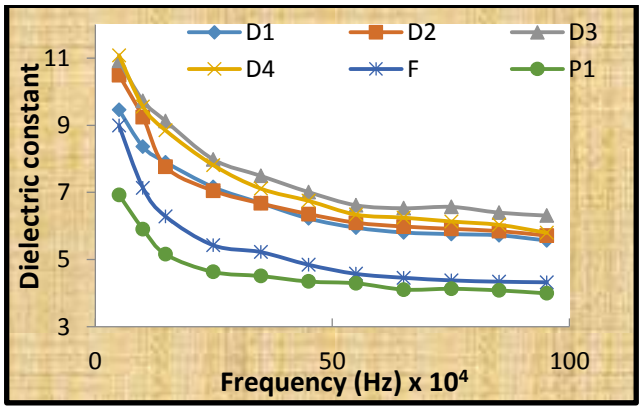

Figure (4): Variation of dielectric constant (ε')with applied frequency for the various samples.

The imaginary part of dielectric constant or named dielectric loss factor was calculated by relation [14]:

$\varepsilon'' = \varepsilon' tan\delta$ Where; $\tan\delta$: is the loss tangent.

Figure (5) appeared the variation of dielectric loss factor ($\boldsymbol{\varepsilon''}$) with applied frequency for the various samples. The decrease in ($\boldsymbol{\varepsilon''}$) with increasing frequency agrees well with Deby's type relaxation process [16]. The dielectric loss factor ($\boldsymbol{\varepsilon''}$) noticed to increase with Ce content because cerium oxide is known as low dielectric loss materials. This indicates that the doped samples as a dielectric ceramic; can store more energy due to small loss and shows good dielectric behaviour[17].

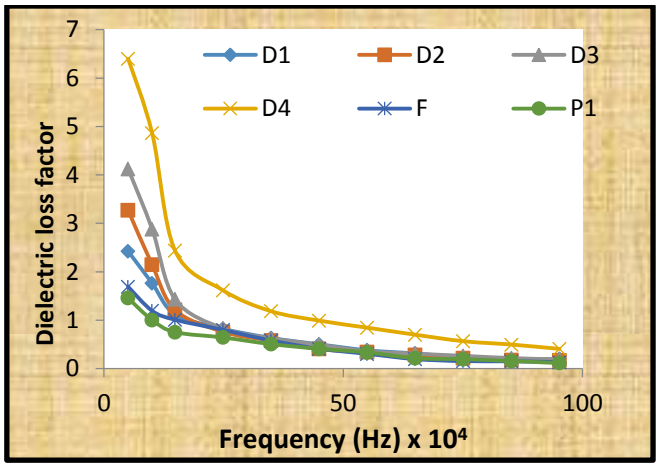

Figure (5): Variation of dielectric loss factor (ε'') with applied frequency for the various samples

The electrical conductivity (σ_{ac}):[17] ($\sigma_{ac} = \omega\varepsilon_O\varepsilon''$, ω: the frequency) increases with the increasing frequency as shown in figure (6), this is may be due to the dipole polarization i.e., the twirling of dipoles between two equalized equilibrium locales is involved. It is the automatic alignment of dipoles in one of the equilibrium locales that leads to the nonlinear polarization. The overall comportment of conductivity follows the universe dynamic react, which has broadly been noticed in disordered substance like ionically proceeding glasses and also doped crystalline solids, and is generally thought to be reflected in the mechanism of charge carted behavior of charge carriers [18].

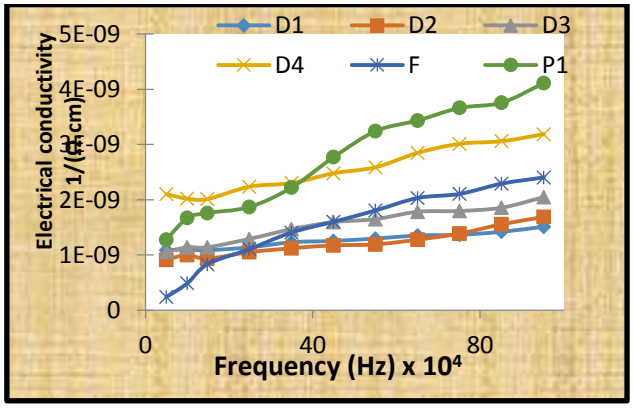

Figure(6) : Variation of Conductivity ($\sigma_{A.c}$) with applied frequency for the various samples

4.3. Initial Magnetic Permeability and Relative Loss Factor

The initial magnetic permeability (μ_i) and relative loss factor (RLF) of all samples were examined by using LCR. The value of (μ_i) was calculated by using the formula [19]:

$$\mu_i = \frac{2\pi L}{2\times10^{-7}\times N^2\times h\times \ln[D_{out}/D_{in}]}$$

Where L: the induction factor, N: the number of turns, D_{out}:Outer diameter of the toroid, the inner diameter of the toroid height of the toroid.

Figure (7) revealed that (μ_i) decreases as the frequency increases and it is influenced by the Ce ion content. D_2 sample has the highest value of (μ_i) , maybe this due to the fact that the grain size would affect directly on the magnetic properties of the ceramic materials. Although the move of the domain wall was impeded by pores and grain boundaries but at less grain boundaries with lower pores and results higher initial permeability by easy motion of domain wall [19,20].

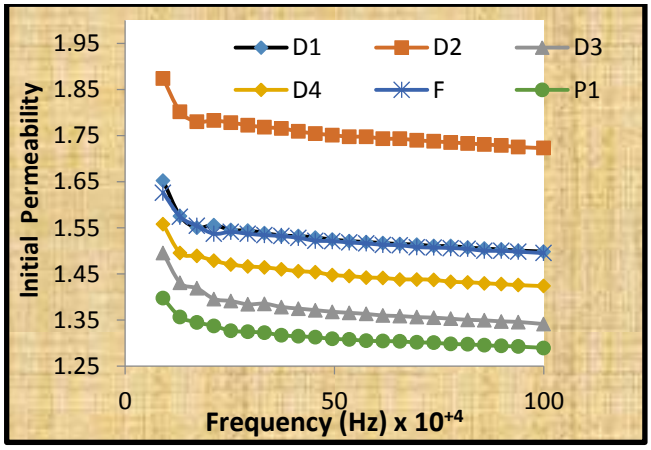

Figure (7) : Variation of initial magnetic permeability (μ_i) with applied frequency for the various samples.

Figure (8) appeared the variation of relative loss factor (RLF) with applied frequency for the various samples. All samples have highest relative loss factor at fewer frequencies, that which may be because to highest hysteresis loss altitude from their porosity structures [21].

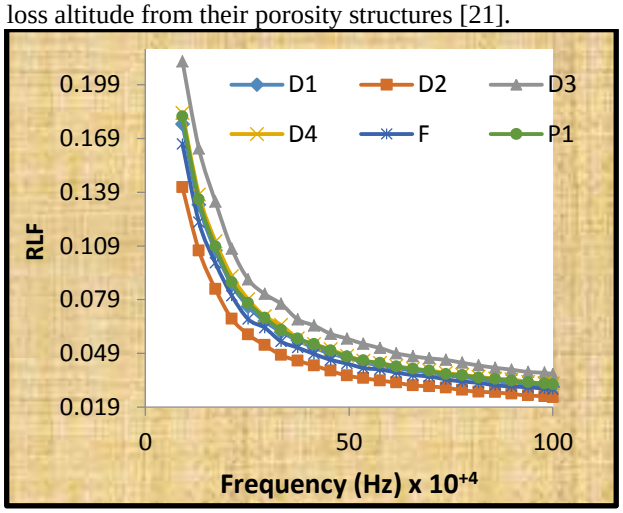

Figure (8) : Variation of Relative Loss Factor with applied frequency for the various samples.

CONCLUSION

($Ce_xFe_{0.05}Mg_{0.95-x}O$) nanoparticles (wherex=0, 0.025, 0.05,0.075 and 0.10) were synthesized by of sol-gel auto–combustion method . XRD results revealed that the prepared samples are polycrystalline in nature with cubic structure. From SEM THE images showed aggregated particles with spherical or semi-spherical shapes and (EDX) analysis revealed the presence of Mg, Ce, Fe and O ions in the synthesized samples. The results revealed that the dielectric loss factor and dielectric constant increase with increasing the content of Ce ion,ion, but the conductivity is inverse that behavior also the results showed that the initial permeability and relative loss factor were affected by changing the content of Ce ion. The $Ce_{0.05}Fe_{0.05}Mg_{0.9}O$ sample showed good crystal structure, fine grain size and good magnetic properties because to high initial magnetic permeability and low loss factor .

REFERENCES

[1] Nirattisai Rakmak, Wisitsree Wiyaratn, Charun Bunyakan, Juntima Chungsiriporn, ,Vol. 162,No.1, pp.84 – 90,(2010).

[2] Zhang, K., An, Y., Zhang, L. & Dong, Q., Vol. 89,No.11, pp. 1414 – 1418,(2012).

[3] Braulio, M.A.L., Brant, P.O.C., Bitterncourt, L.R.M. & Pandolfelli, V.C. , Ceramics International, Vol. 35,No. 8, pp. 3327 – 3334,(2009).

[4] Umar, A., Rahman, M.M. & Hahn, Y., Electrochem Commun, Vol. 11,No. 7, pp. 1353 – 1357,(2009).

[5] Mohd Sufri Mastuli1, Siti Nur Hazlinda Hasbu , Noraziahwati Ibrahim , Mohd Azizi Nawawi , Journal of Analytical Sciences, Vol. 18 ,No. 1,pp. 15 - 20, (2014).

[6] Urvashi Sharma P. Jeevanandam, Journal of Sol-Gel Science and Technology , Vol. 75 , pp. 635-648, (2015).

[7] S. Azzaza, M. El-Hilo , S. Narayanan , J. Judith Vijaya , N. Mamouni , A. Benyoussef , A. El Kenz , M. Bououdina, Journal of Materials Chemistry a, Vol.143, pp. 1500 -1507, (2014).

[8] Sumalin Phokha, Jutharatana Klinkaewnarong, Sitchai Hunpratub, Kornkanok Boonserm, Ekaphan Swatsitang, Santi Maensiri, Journal of Materials Science ,Vol .27,pp. 33-39,(2015).

[9] Toru H. Okabe, Naoto Sato, Yoshitaka Mitsuda and Sachiko Ono, Materials Transactions, Vol. 44, No. 12 pp. 2646 – 2653 (2003).

[10] Samara J. Mohammad, Fadhil Abd Rasin , ,B. Sci. Int. (Lahore), 29(6),1351-1354 (2017).

[11] Khalaf E. Khalil Al- Juboory, College of Education for pure science, University of Tikrit, Vol.21, No.2, pp. 155-61, (2016).

[12] T. Theivasanthi , M. Alagar," Electrolytic Synthesis and Characterizations of Silver Nanopowder ", (2012).

[13] M. Puchalski , P. Dabrowski , W. Olejniczak , P. Krukowski , P. Kowalczyk , K. Ploanski, Journal of materials science-poland, Vol. 2,No. 25 pp.474–478 , (2007).

[14] M. Y. Shahid, A. Anwar, F. Malik, M. Asghar, M. F. Warsi,S. Z. Ilyas, Digest Journal of Nanomaterials and Biostructures Vol. 12, No. 3, July - September, p.p 669 – 677(2017).

[15]K. Kaviyarasu and Prem Anand Devarajan, Journal of Advances in Applied Science Research, Vol.2, No.6, pp.131-138, (2011) .

[16]C. A. F. Vaz, D. Prabhakaran, E. I. Altman,and V. E. Henrich, , Physical Review B 80:155457,pp 1-9,(2009).

[17]Reza Zamiri, Hossein Abbastabar Ahangar, Ajay Kaushal, Azmi Zakaria, Golnoosh Zamiri, David Tobaldi, and J. M. F. Ferreira,,J. PLoS One.; 10(4) :e0122989,(2015)

[18]Pathan Amjadkhan Noorkhan and Sangshetty Kalayne, Journal of Modern Engineering Research (IJMER), Vol.2, pp. 2303-2306,(2012).

[19]Majid Niaz Akhtar, Noorhana Yahya, Patthi Bin Hussain, Journal of Basic & Applied Sciences , vol. 9 ,No.9, pp. 37-40,(2008).

[20]S. Zahi, A. R. Daud, and M. Hashim, Materials Chemistry and Physics, vol. 106, pp. 452-456,(2007).

[21]P. K.Roy, and J. Bera. J. Mat. Pro. Tech., vol. 197, pp. 279-283,(2008).